Part One
Film Growth, Electronic Structure, and Interfaces

Physics of Organic Semiconductors, Second Edition. Edited by Wolfgang Brütting and Chihaya Adachi

1

Organic Molecular Beam Deposition

Frank Schreiber

1.1

Introduction

Organic semiconductors exhibit a range of interesting properties, and their application potential is rather broad, as seen in many other chapters in this book. For the crystalline "small-molecule" systems, grown by organic molecular beam deposition (OMBD), the subject of this chapter, it is generally agreed that the structural definition is important for the functional properties. The following list should serve to illustrate the various aspects:

1) The definition of interfaces (degree of interdiffusion and roughness)
   a) Organic–organic (e.g., in organic diodes)
   b) Organic–metal (e.g., for electrical contacts)
   c) Organic–insulator (e.g., in transistors, insulating layer between gate and semiconductor)
2) The crystal structure
   a) Which structure is present? (Note that polymorphism is very common in organics).
   b) Are different structures coexisting?
   c) Orientation of the structure (epitaxy)?
   d) Is the structure strained (epitaxy)?
3) Crystalline quality/defect structure
   a) Mosaicity (note that in a thin film one has to distinguish between quality in the xy-plane and in z-direction (surface normal)).
   b) Homogeneity within a given film (density of domain boundaries etc.)
   c) Density of defects (and their nature), which also impacts the electronic properties.
4) Issues related to multicomponent systems
   a) Phase segregation versus intermixing; size of "domains."
   b) Possible new structural phases of the mixed system; superstructures?
   c) Tuning of properties by graded concentration profiles?

Physics of Organic Semiconductors, Second Edition. Edited by Wolfgang Brütting and Chihaya Adachi

Since the structure has a strong impact on the functional properties, understanding the structure formation, that is, the growth process, and finding ways to optimize the structural definition is a prerequisite for technological progress. Moreover, understanding the physics of the growth process raises several fundamental challenges.

We will mostly focus on "thicker" films, their growth modes, and the evolution of the morphology for thickness ranges that are typically employed in organic semiconductor applications. We will discuss only to a limited extent the work on the first monolayer, although as the "seed layer" for the following layers this is obviously important. Thus, some of the classical surface science issues, such as binding distances and associated interface dipoles, although very important [1, 2], epitaxial relation, and so on, are not the focus of this chapter. For these issues and also for information on the history of the field, we refer to Refs [3–15]. Also, we will not discuss issues related to chirality, although they are undoubtedly intriguing [11, 16–18].

In terms of growth technology, the equipment is essentially the same as for inorganic molecular beam epitaxy. Evaporation cells on a vacuum chamber are used to provide a flux of molecules at the substrate surface (typically some range around 1 Å/s to 1 Å/min), and ideally the growth can be monitored *in situ*. Virtually, all surface and interface techniques have been used for OMBD-grown films, and we refer to standard textbooks for details of the experimental methodology.

This chapter is organized as follows. We first present some of the general issues in thin film growth and then what is specific and potentially different for organics (Section 1.2). In Section 1.3, we give an overview of the most popular systems. Section 1.4 contains a number of case studies, trying to highlight the issues that we feel are particularly relevant and typical for OMBD. The case studies are based on a few selected compounds and are not intended as an exhaustive list. They are organized according to the (inorganic) substrates, covering, insulators, metals, and semiconductors. In Section 1.7, we briefly indicate the issues for organics-based heterostructures, inorganic–organic, and organic–organic. Some conclusions are given in Section 1.8.

In a review with limited space such as the present one, it cannot be our goal to give a complete and exhaustive overview. Instead, the examples are centered mostly around our own work, which we try to discuss in the context of the general field. This selection is obviously unbalanced, and we apologize for omissions of other important work.

We note that this chapter is an updated version of the 2005 edition of this book and related to Ref. [13]. Important developments since then are, *inter alia*, the precision determination of binding distances of organic semiconductors on metal contacts along with the associated electronic properties (e.g., Refs [1, 2]), the further development of real-time monitoring of growth (e.g., Ref. [19]) and an increased understanding of organic–organic heterostructures, as reviewed at the end of this chapter.

1.2
Organic Molecular Beam Deposition

1.2.1
General Concepts of Thin Film Growth

Crystal and thin film growth are enormously rich subjects with many different facets and theoretical approaches. For a thorough treatment of the underlying concepts, we refer to Refs [20–23]. Here, we shall only briefly touch upon selected aspects that we feel are important in the present context and help to appreciate the issues related to thin film growth (see also Figure 1.1).

One approach to describe the various relevant interactions uses the concept of surface and interface energies, γ, similar to what is done for wetting phenomena. Typically, the surface energies (i.e., the relative contributions of the free substrate surface, γ_s, the film surface, γ_f, and the film–substrate interface, γ_i) are then related to the different growth modes, that is, Frank van der Merwe (layer by layer), Stranski–Krastanov (layer plus islands after a certain critical thickness), and Vollmer–Weber (islands starting at the first monolayer).

We will not discuss issues related to the epitaxial relation in much detail. (For clarity, we should emphasize that under epitaxial relation we understand the crystallographic relation between film and substrate, which does not necessarily imply smooth film growth). However, we should point out that, generally, the surface energies depend on the strain field induced by the lattice mismatch at the film–substrate interface, and thus also on the number of layers of the film. Therefore,

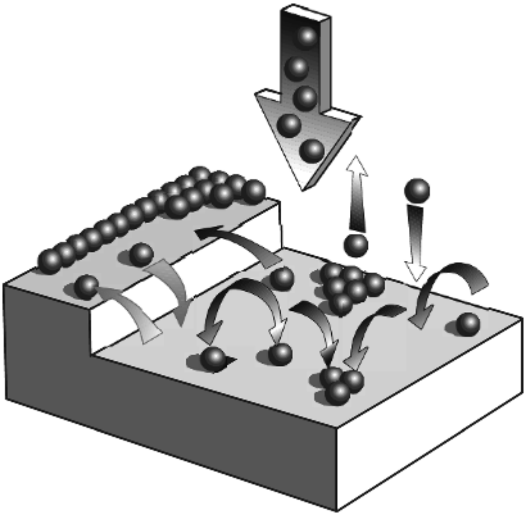

Figure 1.1 Schematic of processes relevant in thin film growth, such as adsorption (as a result of a certain impingement rate), (re-)desorption, intralayer diffusion (on a terrace), interlayer diffusion (across steps), nucleation, and growth of islands.

the epitaxial relation of film and substrate is important not only in a crystallographic sense but also for the growth behavior.

It should be emphasized that growth is actually a nonequilibrium phenomenon, and equilibrium or near-equilibrium energy considerations alone cannot properly account for all growth scenarios. Thus, a dynamic description is needed. This description has to take into account the flux of adsorbates toward the surface (corresponding to a certain supersaturation), the adsorption and redesorption probabilities, and the diffusion processes on the surface (interlayer and intralayer) and their respective barriers. In the past two decades, a theoretical framework has been established, which relates growth mechanisms to a set of scaling exponents describing the dependence of the surface roughness on film thickness and lateral length scale. Much effort has been spent to theoretically predict scaling exponents for certain growth models, as well as to determine them experimentally [20–25].

The scaling theory of growth-induced surface roughness is based on the behavior of the height difference correlation function (HDCF), the mean square height difference $g(R) = \langle [h(x,y) - h(x',y')]^2 \rangle$ of pairs of points laterally separated by $R = \sqrt{(x-x')^2 + (y-y')^2}$. The HDCF displays distinct behaviors for $R \ll \xi$ and $R \gg \xi$, where ξ denotes the correlation length. For $R \ll \xi$ one expects a power law increase as $g(R) \approx a^2 R^{2\alpha}$, where α is the static roughness exponent and the prefactor a is a measure of the typical surface slope. For $R \gg \xi$ the heights at distance R become uncorrelated. Hence, $g(R)$ saturates at the value $g(R \gg \xi) = 2\sigma^2$, where $\sigma = \langle (h - \langle h \rangle)^2 \rangle^{1/2}$ is the standard deviation of the film height (or "rms roughness"). The three parameters σ, ξ, and a evolve with film thickness according to the power laws $\sigma \sim D^{\beta}$, $\xi \sim D^{1/z}$, and $a \sim D^{\lambda}$, defining the growth exponent β, the dynamic exponent z, and the steepening exponent λ. Assuming that the regimes $R \ll \xi$ and $R \gg \xi$ are connected through a scaling form $g(R) = 2\sigma^2 \tilde{g}(R/\xi)$, it follows that the scaling exponents are related by $\beta = \alpha/z + \lambda$. For $\lambda = 0$ (no steepening) one has $\beta = \alpha/z$. Scaling with $\lambda > 0$ is referred to as *anomalous* [22]. The HDCF can be determined experimentally by real space methods (such as atomic force microscopy) or diffuse scattering, each having their advantages [25].

1.2.2
Issues Specific to Organic Thin Film Growth

While the general considerations presented above apply to both inorganic and organic thin-film systems, there are a few issues specific to organics (Figure 1.2), which can lead to quantitatively and qualitatively different growth behavior.

1) Organic molecules are "extended objects" and thus have *internal degrees of freedom*. This is probably the most fundamental difference between growth of atomic and growth of organic systems.
    a) The *orientational degrees of freedom* that are not included in conventional growth models can give rise to qualitatively new phenomena, such as the

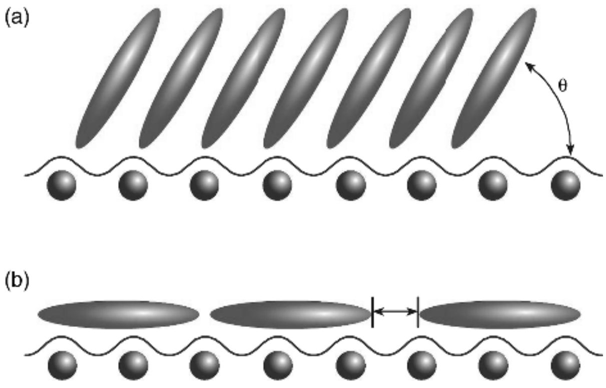

Figure 1.2 Issues specific to organics in the context of thin film growth. (a) Orientational degrees of freedom, potentially leading to orientational domains (additional source of disorder). They can also give rise to orientational transitions during growth. (b) Molecules larger than the unit cells of (inorganic) substrates, thus leading to translational domains. Generally, this can also lead to a smearing-out of the corrugation of the substrate potential experienced by the adsorbate.

change of the molecular orientation during film growth (Figure 1.2). Also, even without considering a *transition* during the growth, the distinction of "lying-down" and "standing-up" films is important and obviously only possible for molecular systems.

   b) The *vibrational degrees of freedom* can have an impact on the interaction with the surface as well as the thermalization upon adsorption and the diffusion behavior.

2) The *interaction potential* (molecule–molecule and molecule–substrate) is generally different from the case of atomic adsorbates, and van der Waals interactions are more important.
   a) The response to strain is generally different. Potentially, more strain can be accommodated, and in those systems where the build-up of strain leads to a "critical thickness" (before the growth mode changes), this thickness can be greater for "softer" materials.

      The different ("softer") interactions with the substrate and the corrugation of the potential have also been discussed in terms of "van der Waals epitaxy" and "quasi-epitaxy."
   b) The importance of van der Waals interactions implies that the relevant temperature scales (both for evaporation from a crucible and for diffusion on the substrate) are usually lower. It should be emphasized, however, that the *total* interaction energy of a molecule (integrated over its "contact area" with a surface) can be substantial and comparable to that of strongly interacting (chemisorbing) atomic adsorbates. Nevertheless, in terms of interaction energies *per atom*, the organic molecules considered here are usually weaker.

   c) Since we are concerned usually with closed shell molecules and van der Waals-type crystals, there are no dangling bonds at the organic surface, and the surface energies are usually weaker than for inorganic substrates.
   d) Importantly, however, if the surface of the *substrate* is "strongly interacting," this results in limited diffusion and thus the evolution of well-ordered films is hampered. In the extreme case of a "very reactive" surface (e.g., with dangling bonds available), the molecules may even dissociate upon adsorption.

3) The *size of the molecules and the associated unit cells* are greater than that of typical (inorganic) substrates.
   a) The effective lateral variation of the potential is smeared out (i.e., averaged over the size of the molecule), making the *effective corrugation* of the substrate as experienced by the molecule generally *weaker* than for atomic adsorbates.
   b) The size difference of the unit cells of adsorbate and substrate implies that there are more translational domains (see Figure 1.2).
   c) Moreover, organics frequently crystallize in low-symmetry structures, which again can lead to multiple domains (not only translational but also orientational domains). Importantly, both are a source of disorder, *in addition* to those known from inorganic systems (e.g., vacancies).

Generally, most of the above points directly or indirectly impact the interactions and thus also the barriers experienced during diffusion. Thus, not only the static structure but also the growth dynamics exhibit differences compared to inorganic systems.

1.2.3
Overview of Popular OMBD Systems

Organic chemistry provides obviously a vast number of dyes and semiconductors, which are potentially interesting for thin film studies, and there is the additional possibility of specifically modifying certain functionalities. A fairly large number of compounds has indeed been employed for thin film work, but not for all of these have detailed growth studies been performed. We will limit ourselves to only selected systems, largely based on examples from our own work (see Figure 1.3).

1.2.3.1 **PTCDA**

The perylene-derivative PTCDA (3,4,9,10-perylene-tetracarboxylic dianhydride, $C_{24}H_8O_6$, a red dye) has long been regarded as a model system for OMBD [4, 5, 26–33]. Its bulk structure (actually α and β phase) exhibits layered molecular planes, and it was expected that the regular stacking of these planes (along the [102] direction in α phase notation) is favorable for well-behaved film growth, which turned out to be not necessarily correct. The optical properties [34–38] and the vibrational properties [38–41] have been thoroughly studied.

1.2.3.2 **DIP**

Diindeno(1,2,3,-*cd*,1′,2′,3′-lm)perylene ($C_{32}H_{16}$, DIP, a red dye) has the same perylene core as PTCDA. It has been shown to exhibit interesting out-of-plane

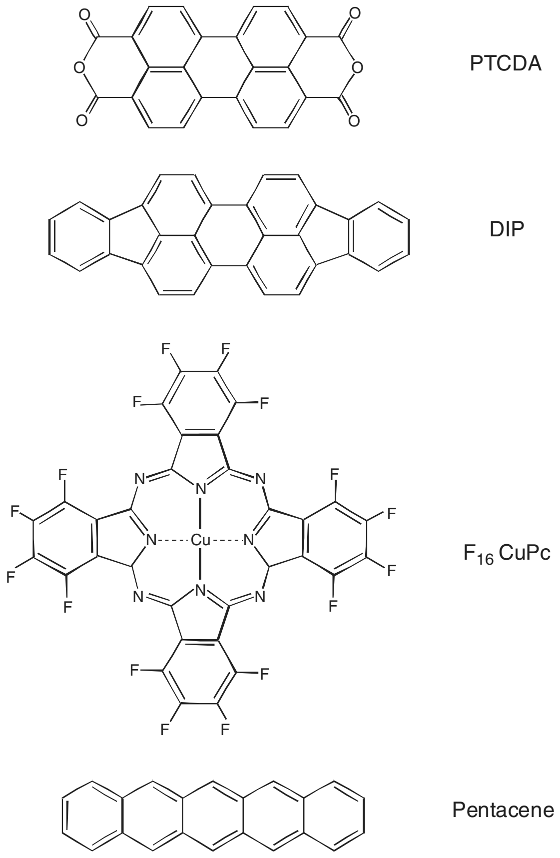

Figure 1.3 Some popular organic semiconductors discussed in this chapter.

ordering behavior [25, 42–44] and, associated with this, good charge carrier transport properties [45, 46]. Recently, its spectroscopic behavior was analyzed in detail [47, 48], and it was also demonstrated to be very promising in OPV devices [49].

1.2.3.3 **Phthalocyanines**

Phthalocyanines (Pc's) are rather popular [50–55], and some of the early work on OMBD has employed Pc's [50]. They exhibit a certain degree of "specific tunability," both due to the possible central metal ion, which can be changed within a broad range, and due to the choice of the side group(s) [51, 52]. F_{16}CuPc is particularly attractive, since it is considered a good candidate as an n-type conducting organic material [56]. As a blue dye [54], it is also interesting for optoelectronic applications [51, 55].

1.2.3.4 Oligoacenes (*Anthracene, Tetracene, and Pentacene*)

The oligoacenes and in particular pentacene have attracted considerable attention, since their charge transport properties were reported to be excellent [9, 45]. An important feature of pentacene seems to be that it can be grown in well-ordered thin films, although the "bulk structure" and a "thin film structure" appear to be competing. A recent development is the synthesis of perfluoropentacene (PFP) [57], which exhibits structural similarities to pentacene (PEN), but electronically of course different [58–61], and allows the preparation of mixed films (see Section 1.7).

There are, of course, many other popular systems. These include, for example, oligothiophenes, oligophenyls, and also "sheets of graphite." Besides the crystalline systems, there are amorphous small-molecule organic semiconductors prepared by OMBD, such as Alq_3 and TPD. In terms of the growth physics, amorphous systems exhibit obviously some differences (no strain due to epitaxy, different diffusion barriers, no crystallographic domains, etc.). They are worth studying in their own right, but we cannot discuss them here. Another interesting case is rubrene, which can form crystals, but for conventional thin-film deposition results in amorphous structures. For examples from various other systems, we refer to Refs [3–15].

1.3
Films on Oxidized Silicon

Silicon wafers are among the most common substrates for thin film growth. They are stable in air with their oxidized surface layer, the thickness of which can be "tuned" by thermal oxidation (from some 15 Å, native oxide, to several 1000 Å). Also, they are very flat and relatively easy to clean.

In the context of organic electronics, of course, they are very popular as substrates for thin-film transistors (TFTs), since the oxide can serve as the insulating layer between the silicon as the bottom contact (gate) and the active organic semiconductor on top.

We should also mention that oxidized silicon surfaces are suitable for surface modification using self-assembled monolayers (SAMs) [62, 63], which has been exploited, for example, for the growth of pentacene [64] and other systems [61].

1.3.1
PTCDA

It was expected that the regular stacking of PTCDA molecules in the [102] direction (in α phase notation) of the bulk structure would give rise to well-behaved film growth. This regular stacking is indeed observed on silicon oxide and many other substrates, unless the growth temperature is too low and no well-defined structure evolves or a too strong interaction with a very "reactive" substrate leads to other orientations of the first PTCDA monolayer. However, it is important to realize that a regular stacking and well-defined orientation of the molecules within the films does not necessarily imply smooth surfaces.

In an early study, it was already found that PTCDA on oxidized silicon exhibits smooth surfaces only for growth at low temperatures ($T < 50\,^\circ\mathrm{C}$ for deposition rates around 1 Å/s), where the crystallinity was not very good [65]. For growth at higher temperatures, the films exhibited good crystallinity, but showed a tendency to island growth ("dewetting").

These results demonstrate a not uncommon feature of growth on substrates with low surface energies. If the films tend to dewet from the substrate near equilibrium, then the above pattern (relatively flat, but low-crystallinity films for low T, and dewetting, that is, rough, morphologies with good crystallinity for high T) is quite frequently found.

1.3.2
DIP

DIP has the same perylene core as PTCDA, but the indeno end groups instead of the anhydride end groups give rise to a completely different structural behavior compared to PTCDA. DIP has been studied in detail both structurally [19, 25, 42–44, 66, 67] and spectroscopically [47, 48, 68–70], and it was found to exhibit excellent out-of-plane order on silicon oxide surfaces.

Films with various film thicknesses ($69\,\text{Å} \leq D \leq 9000\,\text{Å}$) were prepared on oxidized (4000 Å) Si(100) substrates at a substrate temperature of $145 \pm 5^\circ\mathrm{C}$ and at a deposition rate of 12 ± 3 Å/min. The out-of-plane X-ray spectra exhibit well-defined Bragg reflections corresponding to a lattice spacing of $d_{\mathrm{DIP}} \approx 16.55$ Å (suggesting essentially upright-standing molecules) and associated Laue oscillations, the analysis of which shows that the films are coherently ordered across the entire thickness [42]. The rocking width, which is a measure of the distribution of the out-of-plane lattice planes, is 0.01° and lower [42, 44]. The lattice spacing is consistent with a model of molecules standing essentially upright with a tilt angle θ_{tilt} presumably around 15–20°. The large number of higher order Bragg reflections could be used to deconvolute the out-of-plane electron density distribution in a Fourier series (Figure 1.4)

$$\varrho_{el}(z) = \varrho_0 + \sum_n A_n \cos\left(n \frac{2\pi}{d_{\mathrm{DIP}}} z + \phi_n\right) \tag{1.1}$$

where the Fourier amplitude, A_n, is associated with the intensity of the nth Bragg reflection [42]. We can speculate that the shape of DIP with its slightly narrow head and tail may be favorable for an ordering mechanism with some degree of interdigitation of molecules from neighboring (i.e., top and bottom) lattice planes.

On silicon oxide, the in-plane structure is, of course, a 2D powder. The packing appears to follow a herringbone motif. The structure will be discussed also in the context of growth on Au (Ref. [43] and Section 1.5).

The growth including the evolution of the HDCF and the associated growth exponents, α, β, and $1/z$, were studied using AFM and X-ray scattering (specular and diffuse) [25]. Whereas the static roughness exponent α (average of AFM and X-rays 0.684 ± 0.06) is similar to that observed in many other growth experiments [21],

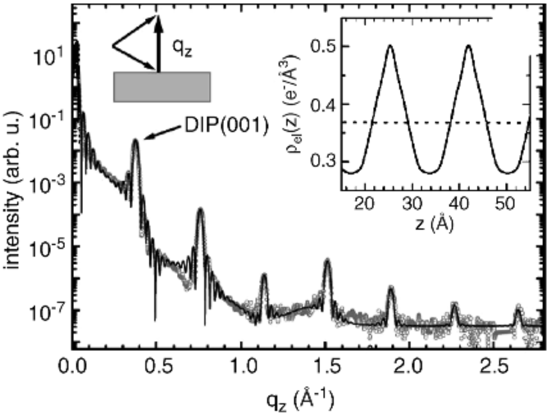

Figure 1.4 Specular X-ray scan of a 206 Å thick DIP film. Many higher order Bragg reflections are observed, which can be used for the reconstruction of the electron density profile using the various Fourier components (close-up shown in the inset). Adapted from Ref. [42].

the values for $1/z$ (0.92 ± 0.20) and β (0.748 ± 0.05) were found to be rather large (Figure 1.5). Specifically, the DIP films belong to the class of systems that display the phenomenon of *rapid roughening*, for which $\beta > 1/2$, that is, the roughness increases faster with thickness D than the random deposition limit $\beta_{RD} = 0.5$ [22]. This effect appears hard to rationalize in the absence of a thermodynamic driving force (e.g., dewetting). A model that is consistent with the scaling exponents involves random spatial inhomogeneities in the local growth rate, which are fixed during the growth process [25, 71]. It is plausible that when certain regions of the

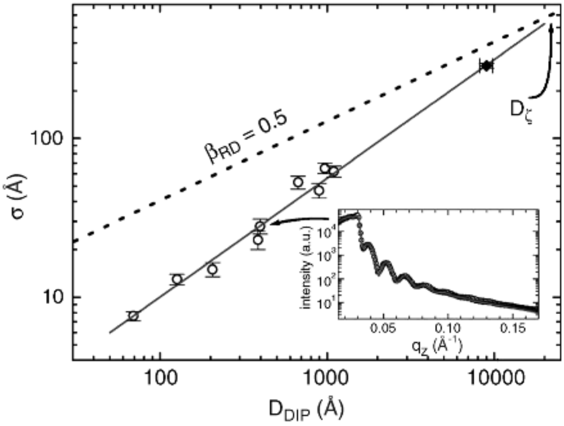

Figure 1.5 Root mean square roughness σ of DIP films as a function of thickness D_{DIP}. The inset shows a typical X-ray reflectivity data set and a fit to the data. The solid line in the main plot is a linear fit to the data and the growth exponent is obtained as $\beta = 0.748 \pm 0.05$. The dotted line denotes the random deposition limit $\beta_{RD} = 0.5$. Adapted from Ref. [25].

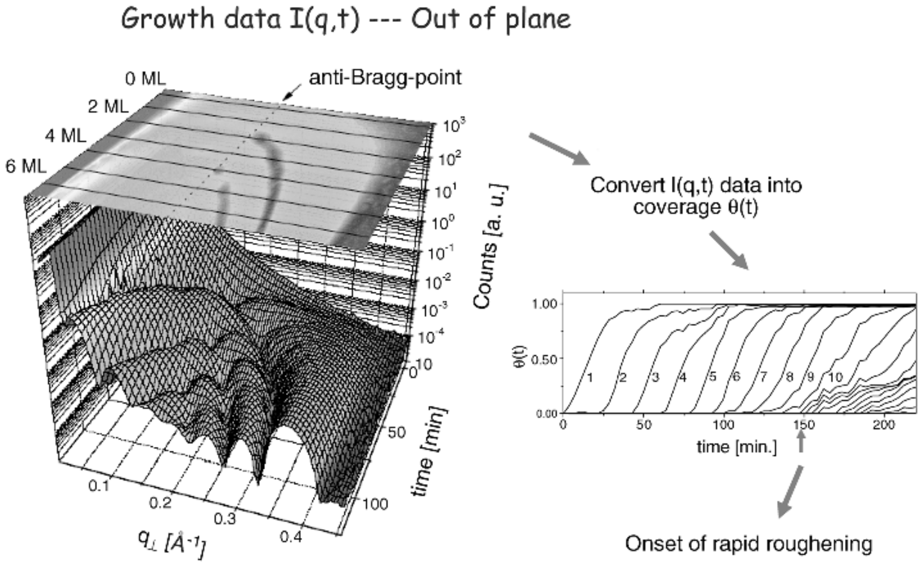

Figure 1.6 (a) The DIP molecule and a schematic of standing (σ) and lying (λ) structures. (b) Evolution of the real-time X-ray reflectivity as a function of time (i.e., film thickness) during growth on silicon oxide (at 130 °C). (c) Layer coverages $\Theta(t)$ as obtained from fits to the above real-time data. A change from layer-by-layer growth to rapid roughening is clearly discernible after about 10 ML (see arrow). Adapted from Ref. [19].

surface persistently grow faster than others, the surface will roughen very rapidly. It was suggested that the spatial inhomogeneities might be related to the different tilt domains of the film and the inevitable grain boundaries in between these [25].

Recently, these issues were followed by X-rays and optical spectroscopy in real-time *in situ* during growth [19, 72, 69] (Figure 1.6), and also steps made visible optically using near-field microscopy with a resolution as good as 17 nm [70].

1.3.3
Phthalocyanines

Phthalocyanines also tend to grow in a standing-up configuration in thicker films on "inert" substrates. Films of $F_{16}CuPc$ between 120 and 450 Å were recently found to exhibit very good crystalline out-of-plane order with rocking widths around 0.01° and well-defined Kiessig interferences and Laue satellites around the out-of-plane Bragg reflection [73].

The in-plane structure is, of course, azimuthally disordered, since the substrate is isotropic. One of the complications for phthalocyanines is a strong anisotropy of the crystal structure and the associated growth properties, which can lead to needle-like features, both for $F_{16}CuPc$ [74] and for $H_{16}CuPc$ [75]. The structure and the optical properties were recently studied in real time [74, 75] revealing changes during growth. Anomalous scaling behavior and surface roughening for H_2Pc deposition were studied in Ref. [76].

1.3.4
Pentacene

Pentacene on silicon oxide has been studied intensely due to its relevance for OFETs, and it is impossible to provide a complete list of references here [9]. Ruiz *et al.* studied the initial stages of the growth [77]. Their analysis of the island distribution in (sub)monolayer films by dynamic scaling showed that the smallest stable island consisted of four molecules. Meyer zu Heringdorf *et al.* showed that under appropriate growth conditions the single-crystal grain sizes can approach 0.1 mm [78].

For thicker films, pentacene thin films exhibit some complication in the sense that there is a "thin film structure" and a "bulk structure," which can coexist, depending on the growth conditions. Also, the defect structure is of interest [79]. Some light was shed on these issues in real-time growth studies [80, 81].

An interesting idea is that of surface modification involving self-assembled monolayers [63]. Shtein *et al.* studied the effects of film morphology and gate dielectric surface preparation on the electrical characteristics of organic vapor-phase-deposited pentacene thin-film transistors including surface modification using SAMs [64]. Meyer zu Heringdorf *et al.* employed cyclohexene saturation of Si(001) to modify the growth dynamics [78]. Voigt *et al.* studied the growth of tetracene on oil-covered surfaces [82]. While they actually used ITO as solid substrates, the concept might equally well be applicable to silicon oxide surfaces.

1.4
Films on Aluminum Oxide

Interfaces of organics with insulators are of obvious relevance for organic electronics, and aluminum oxide is one of the most commonly used insulators. Unfortunately, sputtered aluminum oxide layers frequently exhibit a rather high roughness and not well-defined starting conditions for growth studies. Sapphire is aluminum oxide (Al_2O_3) in its purest and best ordered form. It is also a popular substrate for epitaxy of metals and inorganic semiconductors, and it can be obtained in very high crystalline quality. We will focus here on sapphire, since it is very suitable for model studies of the growth of organics on insulator surfaces (see Section 1.6 for other substrates).

Surfaces of ionic substrates, which are not charge balanced, tend to be unstable and/or exhibit strong relaxations/reconstructions. In the case of sapphire, the $(11\bar{2}0)$ surface ("A plane") is charge balanced and rather inert, and it has been used for growth studies. An important feature to realize for surfaces of crystals is that they commonly exhibit a miscut, that is, a difference between the physical surface

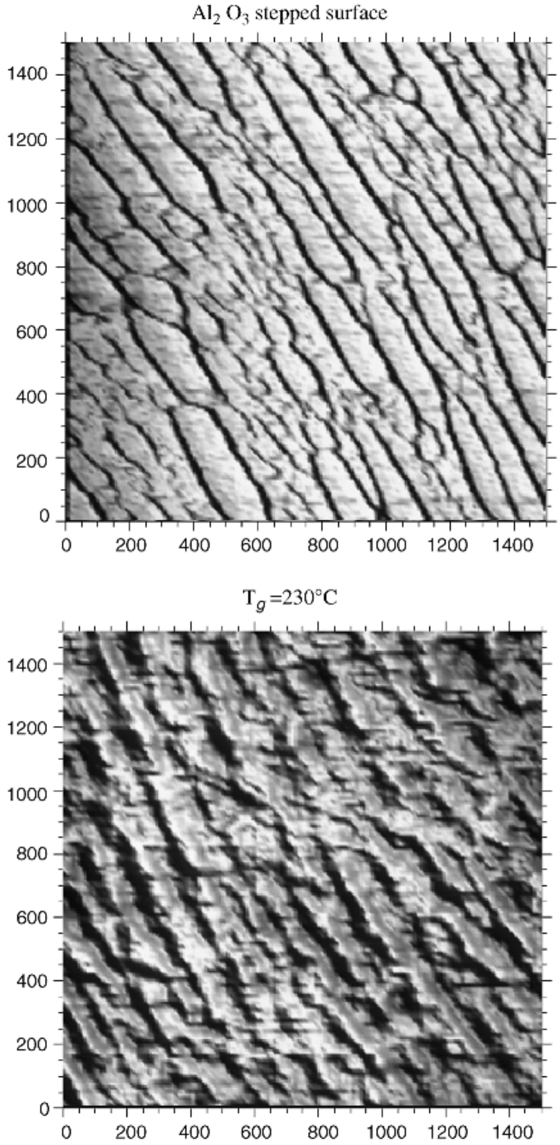

Figure 1.7 Topography of an A-plane sapphire substrate (*top*) and an $F_{16}CuPc$ film (120 Å) (*bottom*) on this substrate determined by noncontact AFM. The step pattern of the substrate serves to azimuthally align the film (see text). Adapted from Ref. [84].

and the (low-index) crystallographic plane. This gives rise to a step pattern, which in the case of essentially perfect crystals like sapphire is the dominating feature of the surface morphology (Figure 1.7). Issues related to the surface preparation have been discussed in Ref. [83].

1.4.1
PTCDA

PTCDA on sapphire has, to our knowledge, not been studied in detail. Test results, however, indicate that the overall behavior is similar to that for PTCDA on oxidized silicon, that is, for growth at high temperatures the films tend to (partially) dewet (Krause et al., unpublished).

The overall growth scenario is most likely not changed significantly by the presence of steps, but the in-plane order of PTCDA may be affected. However, even with alignment at the step edges, PTCDA would most likely still exhibit multiple domains (see also the discussion of PTCDA on metals).

1.4.2
DIP

Based on the results for DIP on silicon oxide it is expected that DIP would also exhibit good out-of-plane ordering on the similarly “inert” sapphire. Preliminary data indicate that this is, in fact, the case (Osso et al., unpublished). In addition, the stepped sapphire substrate can induce in-plane ordering, as first demonstrated for the growth of phthalocyanines [84] (see below), which was also found for DIP (Osso et al., unpublished).

1.4.3
Phthalocyanines

As described above, the regular surface steps associated with miscut sapphire can serve as templates for film growth with azimuthal alignment. While the concept of stepped substrates has been used frequently for monolayer adsorbates, its use for comparatively thick films (5–50 ML) of relatively large molecules was first demonstrated by Osso *et al.* for F_{16}CuPc on A-plane sapphire [84]. The resulting azimuthal ordering has been shown by four methods sensitive to different aspects of order [84]. AFM was used to image the surface morphology of the bare substrate. After film growth, the characteristic step pattern of the bare substrate was shown to be basically replicated, suggesting an azimuthal coupling of the film structure to the substrate morphology (Figure 1.7). In-plane X-ray diffraction (GIXD) showed that the crystal structure of the film was indeed not a 2D powder, but was aligned. The distribution width (“mosaicity” of the in-plane lattice) was several degrees broad, which suggests a rather soft/weak driving force for the ordering. The in-plane order was also visible in the azimuthal intensity distribution of the vibrational modes detected by Raman scattering. Finally, the resulting anisotropy of the dielectric function was studied by spectroscopic ellipsometry, offering the chance to study the “*intrinsic*” behavior of these systems without a strongly reduced disorder-induced broadening of the optical transitions. We should note that the strong optical anisotropies of these systems are an interesting field of study in their own right, and give rise to nontrivial effects in the propagation of light [54].

The out-of-plane ordering was similarly good for $F_{16}CuPc$ or DIP on silicon oxide, that is, a well-defined Bragg reflection with Laue oscillations and mosaicities around 0.01°, although the tendency of phthalocyanines to grow in needles can cause some complications. We note that the tilt angle of the molecules as well as the out-of-plane lattice parameter was found to depend on the growth temperature (and are different from the bulk structure parameters), indicating that the structure may not be in full equilibrium.

1.4.4
Pentacene

Similar concepts and mechanisms as observed for DIP and $F_{16}CuPc$ in terms of azimuthal alignment should be applicable to pentacene on sapphire, but to our knowledge there are no published results yet.

1.5
Films on Metals

Interfaces with metals are of obvious relevance for contacting organic semiconductors. The choice of the metal is frequently determined more by the desired work function and thus electron or hole injection properties than by growth considerations. Nevertheless, there are a wide variety of metals in terms of behavior as substrates for organic thin film growth, and it is important to realize that this can have a profound impact on the growth and the resulting structural and functional properties. Besides issues related to the surface morphology, crystalline quality, potentially crystalline orientation, and size of the unit cell (epitaxy), it is very important how "reactive" or "inert" the metal is, since this determines the mobility of the molecules on the surface and thus the growth.

For strongly reactive substrates, the molecules tend to behave almost in a "hit-and-stick" fashion, that is, without significant mobility and thus no long-range order. Less reactive metals such as noble metals, to which we will limit ourselves here, turned out to be rather popular and suitable.

We will concentrate on metal single crystals. From a practical point of view, for growth studies it is important that their surfaces can be "recycled" by sputtering and annealing, that is, several growth experiments can be performed on the same substrate and on (essentially) the same surface. Less reactive metals are also easier to keep clean before growth. Obviously, with metal substrates the application of electron-based surface science methods is possible, since the signal does not suffer from charging effects. This has been used excessively by the surface science community in particular for molecular monolayers on surfaces of metal single crystals.

We should also mention that metal surfaces are suitable for surface modification using SAMs [62, 63], which has been employed in particular for Au(111). Examples include the growth of PTCDA on alkanethiol SAMs [85–88].

1.5.1
PTCDA

PTCDA on metal surfaces has been thoroughly studied, with the noble metals being particularly popular.

1.5.1.1 Structure and Epitaxy of PTCDA/Ag(111)

On Ag(111), well-defined epitaxial growth of PTCDA(102) has been observed [4, 26, 30, 32]. The 2D structure is characterized by a herringbone arrangement of the flat-lying molecules, which corresponds to a layer of the (102) plane of the bulk structure, with a small degree of distortion (strain). Possible mechanisms leading to the well-behaved 2D structure of PTCDA on Ag(111) were discussed in Ref. [89]. The vertical PTCDA-Ag(111) spacing was found to be 2.85 ± 0.1 Å based on X-ray diffraction [31], but it may differ for low-temperature deposition if the adsorption state differs. Subsequently, still more precise and even element-resolved vertical bonding geometries of PTCDA monolayers were determined using XSW [90, 91].

Overall, in particular monolayers of PTCDA on Ag(111) have been studied in detail using a broad range of techniques; for a collection of references see Refs [92, 93].

For growth extending beyond the monolayer, a more complex azimuthal distribution arises, and, depending on the growth temperature, also domains noncollinear with principal axes of the substrate can form to relieve strain [30]. Interestingly, the epitaxial relations could be rationalized similar to the Nishiyama–Wassermann versus Kurdjumov–Sachs relations for fcc(111)/bcc(110) growth, although the PTCDA structure is not bcc [30].

We note that PTCDA/Ag(111) has also been subject of a number of spectroscopic studies. One of the challenges is understanding the molecule–substrate interaction, which is “between pure van der Waals and clear covalent binding.” Details are beyond the scope of this chapter (see Ref. [93] and references therein).

1.5.1.2 Comparison with Other Substrates

The comparison with PTCDA/Au(111) yields a qualitatively similar picture [28, 33, 94], although details of the epitaxy appear to differ, which is not too surprising given that structure is a result of a rather delicate balance of different factors and given that the corrugation of the substrate potential experienced by PTCDA is different.

It is interesting to compare monolayers of PTCDA on different noble metal surfaces. The tendency is as expected from “a stronger chemical interaction” on Cu(111) via the intermediate case on Ag(111) to the weakest interaction on Au(111), which is seen both in the vertical bonding distances and in the valence band spectra [91, 95, 96].

On the more open Ag(110) surface, an entirely different structure already in the monolayer was found, characterized by a “brick-stone” arrangement [26]. Phase transitions of PTCDA/Ag(110) were studied in Ref. [97].

Growth on Cu(110) was studied by Möller's group [98–100]. The monolayer was found to differ from those known from other substrates. For thicker films, Stranski–Krastanov growth was found, similar to the case on Ag(111) (see below).

1.5.1.3 **Dewetting and Thermal Properties**

While the structure and epitaxy in the monolayer regime are well defined, the later stages of the growth (potentially after a certain threshold thickness) can, of course, exhibit islanding and a very rough resulting morphology. It was found that PTCDA on Ag(111), a well-behaved system in the monolayer regime, indeed exhibits Stranski–Krastanov growth. At growth temperatures $T \lesssim 350\,\mathrm{K}$, relatively smooth epitaxial films have been found, whereas at $T \gtrsim 350\,\mathrm{K}$, well-separated crystallites with bulk crystalline structure on top of a 2 ML thick wetting layer have been observed [30, 31, 101, 102]. These results are qualitatively the same as those for PTCDA on Au(111) [28].

The thermally induced post-growth dewetting of "low-temperature" grown films was also studied, confirming that the films tend to dewet if given sufficient thermal energy [31]. In these experiments, the thermal expansion of PTCDA was also determined ($1.06 \pm 0.06\,\mathrm{K}^{-1}$ out of plane) [31]. For a comparison with other systems ($\mathrm{Alq_3}$ and TPD), see Ref. [103]. While islanding of the films is usually not desirable, it should be pointed out there might also be ways to exploit islanding or dewetting and the formation of small crystallites for "self-organized nanostructures" (similar to Si–Ge quantum dots).

1.5.1.4 **Real-Time Growth**

In order to shed light on the dynamics and the temperature dependence of the 2D–3D transition (layer by layer to islanding), a real-time X-ray diffraction study of the growth of PTCDA on Ag(111) was performed [102]. The idea is as follows (Figure 1.8). In kinematic theory the specular X-ray scattering intensity is the sum of the scattering contributions from the film and the substrate,

$$I(q_z, t) = |F(q_z, t)|^2 = \left| f_\mathrm{F} \sum_{n=1}^{\infty} \mathrm{e}^{iq_z d_\mathrm{F}(n-1)} \theta_n(t) + f_\mathrm{S} \frac{1}{1-\mathrm{e}^{-iq_z d_S}} \mathrm{e}^{-iq_z d_0} \right|^2 \tag{1.2}$$

where f_F and f_S are the form factors of the film and the substrate, respectively, d_F and d_S are the corresponding lattice spacings, and $d_0 = 2.8\,\mathrm{Å}$ is the distance between the substrate and the first layer of the film [30]. $\theta_n(t)$ is the time-dependent fractional coverage of the nth layer within the organic film. At the anti-Bragg point of the PTCDA film ($q_z^* = \pi/d_\mathrm{F}$), the first term in Eq. (1.2) equals $f_\mathrm{F} \sum (-1)^{(n-1)} \theta_n(t)$. Therefore, the coverage difference

$$\Delta\theta(t) = \sum_m \theta_{2m+1}(t) - \sum_m \theta_{2m}(t) = \theta_\mathrm{odd}(t) - \theta_\mathrm{even}(t) \tag{1.3}$$

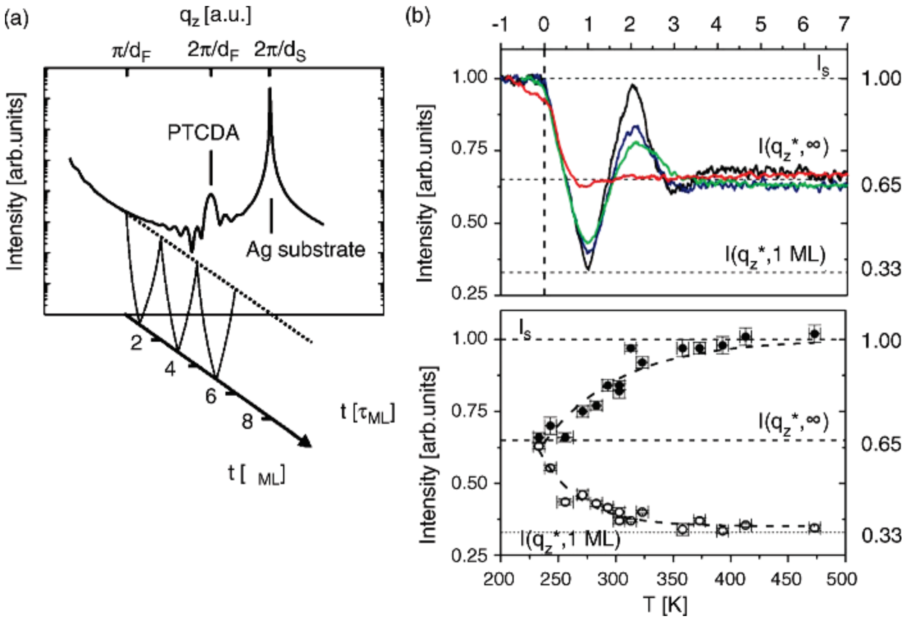

Figure 1.8 Simulation of the specular rod scattering of a thin PTCDA film on Ag(111) as a function of the out-of-plane momentum transfer q_z (*top*). The time axis in this figure (for a fixed q_z) indicates the intensity oscillations at the anti-Bragg point during growth (see text for explanation). The central figure shows the time dependence (in units of monolayer deposition times) of the normalized scattered intensity at the anti-Bragg point for various temperatures (233 K (red), 283 K (green), 303 K (blue), and 358 K (black)). The bottom figure shows the temperature dependence of the deviation from layer-by-layer growth expressed in terms of the intensity of the minimum (open symbols) and of the maximum (filled symbols) of the scattered intensity at 1 ML and 2 ML, respectively (see text for details). Adapted from Ref. [102].

can be deduced from the measured intensity $I(q_z^*, t)$. Specifically, it is possible to distinguish the coverage of the first and the second layer in the initial stage of the growth. In the case of layer-by-layer growth, characteristic intensity oscillations are observed.

Figure 1.8 shows typical time-dependent intensity data during growth in a dedicated chamber [104], measured at various substrate temperatures between 233 and 258 K [102]. $t = 0$ is defined as the starting time of the deposition. The signal is normalized to the substrate scattering intensity, $I_S = I(q_z^*, t < 0)$, and the time is normalized to the deposition time, τ_{ML}, of one monolayer, which corresponds to the intensity minimum. A typical growth measurement exhibits distinct intensity oscillations for $t \lesssim 3\tau_{ML}$, followed by a constant intensity during further deposition, similar to the observations for PTCDA/Au(111) [105]. The intensity oscillations correspond to layer-by-layer growth. The transition to a constant intensity indicates the breakdown of layer-by-layer growth and the onset of islanding characteristic of SK growth. As can be seen from the transition to a time-independent scattering signal (associated with an equal probability for a given molecule to be accommodated in even and odd layers), the islanding starts rapidly after completion of a 2 ML "wetting" layer.

Comparing the growth data for different temperatures (Figure 1.8), we find that for $T \geq 358$ K the oscillations are not visibly damped for $t < 2\tau_{\text{ML}}$. They are followed by a sharp transition to a time-independent intensity (islanding). For lower temperatures, the oscillations are progressively damped, and the 2D–3D transition is smeared out as the temperature is lowered.

The experimental data, that is, in particular the 2D–3D transition, could be modeled by kinetic Monte Carlo simulations using a relatively simple model for the energies/barriers, the most important feature of which is the dependence of the interlayer transport barrier, E_{inter}, on the layer number n, namely, $E_{\text{inter}}(n \leq 3) = 0$ and $E_{\text{inter}}(n > 3) > 0$ [102].

The growth of PTCDA/Ag(111) could also be monitored in real time in real space using PEEM [106]. Moreover, for elevated temperatures strong postgrowth diffusion was observed [107].

1.5.2
DIP

In the monolayer regime, DIP, like many other organic semiconductors, was studied by STM. The molecules were found to be lying down flat on the substrate [108]. The interaction of DIP with Au was found to be physisorptive. In the regime of thicker films, DIP was studied in detail *on* Au contacts [43] (and as substrate for Au contacts evaporated *on* DIP [43, 66–68]). Importantly, in contrast to growth on silicon oxide, due to the stronger interaction with the Au substrate, the lying-down configuration tends to prevail not only for monolayers but also for multilayers. Since the standing-up configuration (which again followed a herringbone-like motif) appears to have the more favorable surface energy (as seen on silicon oxide), there is obviously a competition between the two configurations (standing-up versus lying-down), and they are found to coexist [43]. From the point of view of growth kinetics, this competition is very interesting, but it is certainly a further complication and an additional source of disorder that is usually undesirable. These issues were recently studied using (electronic) spectromicroscopy [109]. Furthermore, mixed films of DIP and CuPc were studied by STM in the monolayer regime [110].

1.5.3
Phthalocyanines

Phthalocyanines were among the first "large" molecules that were studied by STM with (sub)molecular resolution [50]. In the monolayer regime, the molecules lie down flat on the surface, and the 2D structures have been thoroughly studied.

Recently, the (vertical) bonding distance to the metal substrate was determined using XSW [2, 111, 112]. For thicker films, there is a competition between the lying-down configuration of the first layer and the tendency to stand up. The impact of roughness on the ordering behavior was studied in Ref. [113].

1.5.4
Pentacene

Acenes on metal substrates were studied by several groups. Early work on the orientation of various aromatic hydrocarbons including tetracene on metal surfaces using NEXAFS was done by Koch and coworkers [114].

More recent work focused on pentacene. Pentacene structures on Au(111) as a function of coverage (up to the equivalent of around 2 ML) were studied by Parkinson's group [115]. A very detailed study of pentacene on clean and SAM-modified gold surfaces was presented by Käfer *et al.* [116].

The structure and binding distance as well as associated electronic properties such as work function and interface dipole of PEN and also of PFP on Cu(111) were determined with high precision in Ref. [117].

In the monolayer regime of pentacene on Cu(110), Lukas *et al.* reported a novel mechanism giving rise to long-range order on Cu(110), based on the modulation of the adsorption energy due to charge-density waves related to a surface state [118]. While it is not too surprising that the molecules in the monolayer regime tend to be lying more or less flat on the surface, importantly, for the growth of thicker films on Cu(110) an orientational transition from a lying-down configuration to an essentially standing-up configuration was observed [119].

An interesting study of the "hyperthermal" growth of pentacene (exhibiting hyperthermal energies in a seeded supersonic molecular beam) on Ag(111) was presented by Casalis *et al.* [120]. They found that at low substrate temperatures (200 K), highly ordered films can be grown by hyperthermal deposition when thermal deposition leads only to disordered films. The results were interpreted as a result of "local annealing" due to the impact of the hyperthermal molecules. This technique appears to have the potential to tailor the growth of molecular systems in addition to what is possible by changing the impingement rate and the substrate temperature, and it may be further tested in the future (see Ref. [61] for recent work on PFP).

1.6
Films on Other Substrates

Many substrates other than the above ones have been employed, all of which we cannot review. We shall mention only some of the most important other substrates.

Quite popular for growth studies is graphite, since it is easy to prepare. In our general classification of substrates, graphite would be "weakly interacting." For spectroscopic studies, this offers the opportunity to study the film without strong “interference” from the substrate; see, for example, Ref. [121] and references therein. Other examples from this group of layered substrates are MoS_2, GeS, and Sb_2S_3 [6].

Also rather weakly interacting would be MgO, which falls essentially in the same category as sapphire and silicon oxide. Mica, which can be easily prepared by cleavage, may also be seen in the category of rather inert substrates. It can also be used well for real-time differential reflectance spectroscopy (DRS) [122].

Alkalihalogenides, such as NaCl and KCl, are quite popular as simple substrates for growth studies, since they are easy to prepare. For some studies, they have the additional benefit that they can be easily dissolved and the film can be studied by TEM.

Metals, as indicated above, span a broad range from the noble metals to very reactive substrates.

A very important class of substrates are certainly (inorganic) semiconductors such as Si and GaAs, since they may be used in the integration of organic–inorganic hybrid devices. Moreover, they are very well defined in terms of their surface and overall structural quality, which is favorable for growth studies. If the surface is clean, however, they can exhibit “dangling bonds” and be rather reactive. In these cases, the organic adsorbates then tend to “hit and stick,” that is, they usually do not diffuse over significant distances, hence they do not form long-range ordered structures. A strategy to avoid these problems, but still benefit from the above advantages, is the use of surface-passivated semiconductors, such as H–Si or Se–GaAs.

Polymeric substrates and possible routes for oriented growth of pentacene have been studied in Ref. [123].

1.7
More Complex Heterostructures and Technical Interfaces

Organic semiconductor devices frequently do not only consist of a film on a substrate, but involve additional layers such as metal contacts or insulating layers or also different organic components in a multilayer structure.

1.7.1
Inorganic–Organic Heterostructures

Metal contacts are one obvious requirement for many applications of organic semiconductors. It turns out that the controlled deposition of metals *on* organics (“top electrode”) is nontrivial. In order to reduce problems related to interdiffusion (and ultimately short-circuiting) and traps related to surface states, different strategies can be pursued.

1) Deposition at low temperatures to “freeze in” the interdiffusion.
2) Deposition at (moderately) high rates with the idea that the metals are quickly forming larger aggregates that are then less mobile and diffuse less far into the organic film.

3) The use of "suitably reactive" metals and/or organics, so that a strong interaction at the top layer(s) of the organic material prevents interdiffusion.
4) "Soft deposition" by "thermalizing" or at least reducing the energy of the impinging metal atoms by "baffling" these using a noble gas or other means [124].
5) Miscellaneous other nonthermal deposition strategies including, for example, electrochemical deposition may be attempted.

Our group performed studies of the deposition of gold, which is widely used as a hole injection material, onto well-defined DIP thin-film surfaces to study the interdiffusion (Figure 1.9). The study followed the "classical" approach without specific precaution against interdiffusion except for variation in the temperature and the rate [43, 44, 66–68]. The important result was that under rather typical deposition conditions near room temperature, the metal interdiffusion was already significant, and the layers would exhibit electrical shorts (Figure 1.9). If the substrate, however, is cooled, fairly well-defined interfaces could be obtained. We note that Faupel"s group studied similar issues in detail for metal deposition on polymers [125, 126].

Sellner *et al.* [127, 128] have studied aluminum oxide/DIP interfaces, which exhibit a very different interdiffusion behavior. Even the use of aluminum oxide capping layers, giving rise to significantly enhanced thermal stability of the underlying organic layer, are possible and may be used for encapsulation of devices.

We should note that for device structures one also has to take into account the effect of the morphology of technical interfaces and surfaces on the growth behavior of organics [113].

1.7.2
Organic–Organic Heterostructures

Another important interface, which has not been excessively studied with regard to growth and structure, is the organic–organic interface as found, for example, in OLEDs and in OPV devices. Some early work on superlattices and bilayers can be found, for example, in Refs [129–132]. PTCDA on self-assembled monolayers as well-defined organic model surfaces has been studied in Refs [85–88]. PTCDA on hexa-peri-hexabenzocoronene (HBC) was investigated in Ref. [133]. A number of different polynuclear aromatic hydrocarbons including DIP and perylene were studied by Kobayashi's group [134]. Other studies were concerned with the post-growth stability of the organic–organic interface and the interdiffusion behavior [103, 135].

Recently, the study of organic–organic structures has attracted increased interest, and different architectures have been studied in more detail. For an up-to-date review on this specific topic, see Ref. [136].

For A-on-B-type structures, which in device terminology correspond to "planar heterojunctions" (PHJ), in addition to the interface stability, there are other issues.

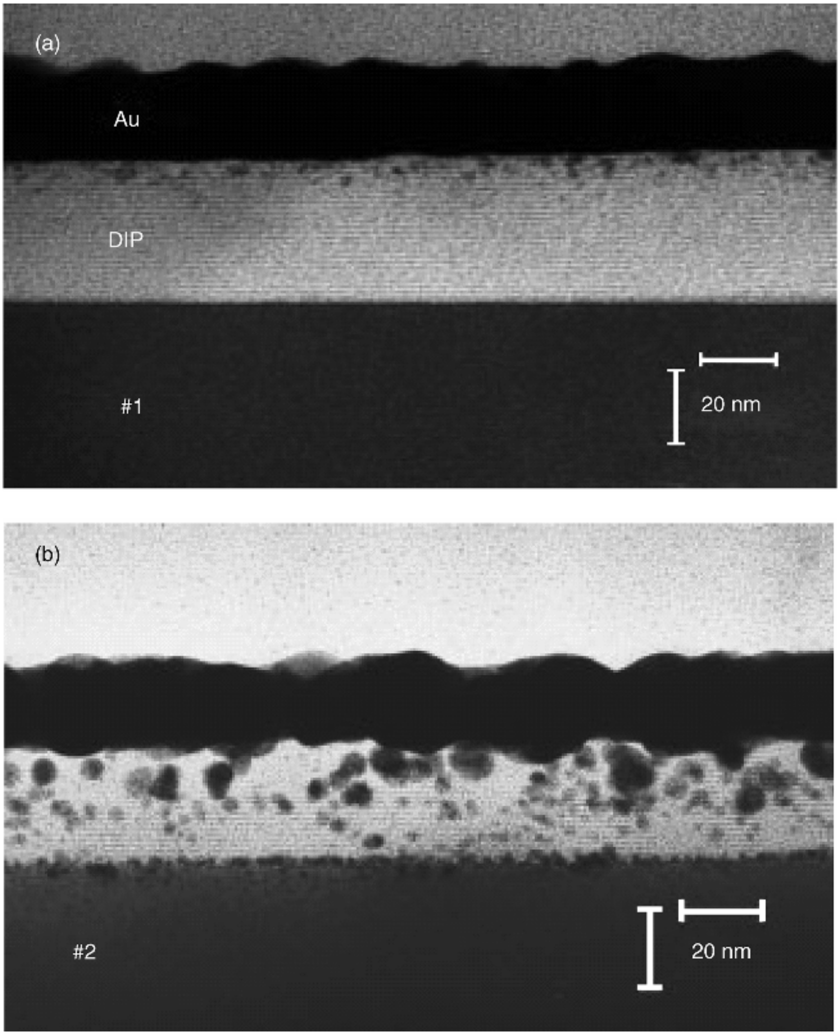

Figure 1.9 Cross-sectional TEM images of two Au/DIP/silicon oxide heterostructures. While the Au contact prepared at −120 °C and at a rate of 23 Å/min (a) exhibits rather well-defined interfaces, the Au contact prepared at 70 °C and at a rate of 0.35 Å/min (b) shows strong interdiffusion. Note that individual lattice planes of the DIP film can be resolved. Adapted from Ref. [66].

One of these issues is related to the evolution of roughness. An interesting effect is smoothing (see Figure 1.10), which was observed for PFP on DIP and PEN on PFP [137]. For both systems, surface smoothing during thermal evaporation of the second material on top of the first is observed. The smoothing can be rationalized by a, compared to homoepitaxy, lowered step edge barrier for one species diffusing on the other, but more details have yet to be explored.

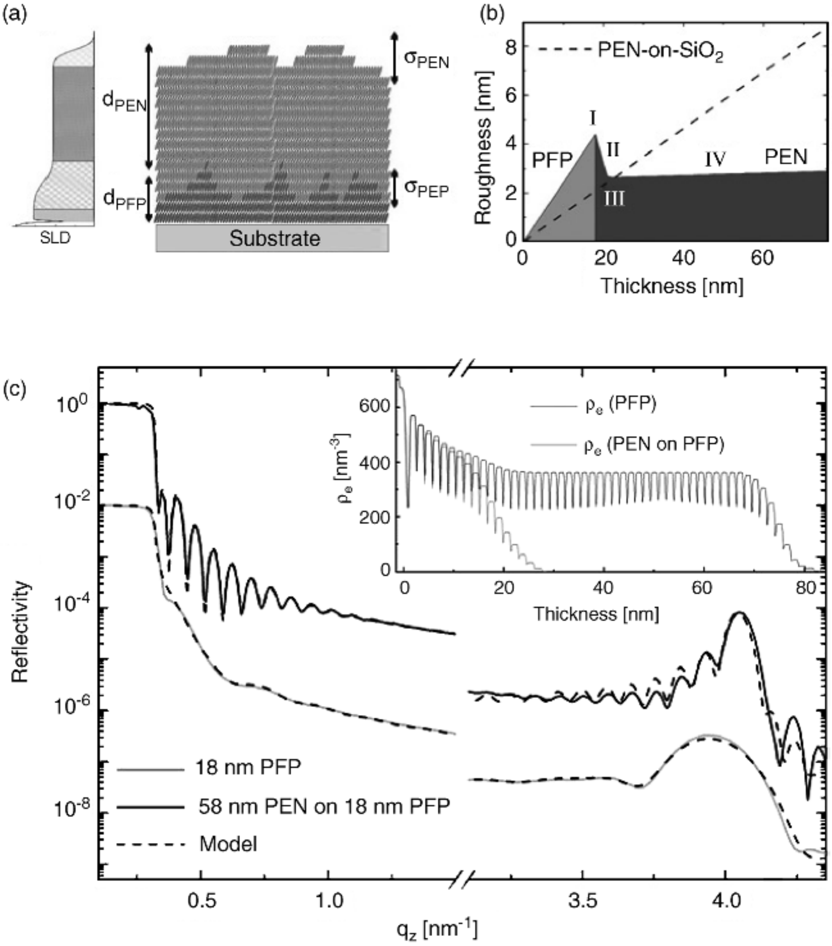

Figure 1.10 (a) Heterostructure with thicknesses of the organic layers d_{PFP} and d_{PEN} and roughness of the intermediate interface σ_{PFP} and the top roughness σ_{PEN}. (b) Roughness evolution during film growth. (c) Reflectivity data and fits from a 18 nm thick PFP film, and from a PEN-on-PFP heterostructure with $d_{PFP} = 18$ nm and $d_{PEN} = 58$ nm. The inset shows ϱ_e for both fits. Adapted from Ref. [137].

In contrast to the above scenario, for the system DIP on $F_{16}CuPc$, Stranski–Krastanov growth was reported [138], underlining that, of course, the growth scenario depends on the specific system.

Another important question concerns the molecular orientation (in particular, "lying down" versus "standing up" for rod-like molecules) at the interface or induced by the interface. The orientation may be changed (compared to single-component film growth on, say, silicon oxide) by an underlying organic layer, for example, by the balance of the interface energies. It may also be influenced by a specific step pattern or its height, which for organics is obviously greater than for typical inorganic substrates. In this context, one may observe templating effects, that is, the growth behavior of the top layer may depend on the structural and morphological properties of the bottom layer. This was demonstrated, for example, for PFP on DIP. Two main effects were observed: PFP molecules in the top layer adopt partly the orientation of the DIP molecules in the bottom layer and the crystalline quality of the PFP layer correlates with the crystalline quality of the DIP layer underneath in terms of the coherent in-plane island size [142].

Apart from the various combinations of PEN, PFP, F_{16}CuPc, and DIP mentioned above, other A-on-B heterostructures were studied [136]. Here, we shall not attempt to provide a complete list but rather refer to other chapters in this book and to the paragraph further below on work relating different architectures to device performance.

For A-mixed-with-B-type structures, in particular coevaporated (50 : 50) films, which correspond to “bulk heterojunctions” (BHJs) in OPV devices, there are several fundamental structural issues to be addressed. First of all, there is the question of intermixing versus phase segregation. As an “ordered form of intermixing,” one may even find the formation of a true superstructure (“A-B-A-B-A- . . . ,” to be seen most directly from a superlattice reflection), in contrast to a “statistical occupancy” of the different lattice sites by A and B [139, 140]. These are classical issues in the physics of metals (ordered versus disordered alloys).

Entropy, which will always favor intermixing, has to be compared to the balance of the interactions (A with A and B with B versus A with B), which then determines whether intermixing is indeed found. In addition to direct (“conventional”) interactions, there are steric issues. For instance, CuPc and C60 are structurally/sterically apparently incompatible (platelet versus sphere), so that an ordered structure and intermixing on the molecular level is not expected, and indeed is not found [49].

A promising system for good intermixing appears to be PEN:PFP, since this may exhibit favorable interactions for intermixing and very little steric difficulties, since the two compounds are derived from the same molecular structure. Consequently, the system PEN:PFP was studied in detail both structurally [139, 141] and spectroscopically [142–144]. Indeed, it could be shown that PEN:PFP does tend to intermix and form its own structure with 1 : 1 stoichiometry. However, the situation for continuous variation in the composition is actually rather complex. Scenarios with different coexisting structures are possible, for example, if the structure with 1 : 1 stoichiometry is favorable, for compositions different from 1 : 1, the “ordered 1 : 1 regions” may coexist with regions with excess molecules of one or the other compound, if there is no “continuous intermixing.” For a detailed discussion of the subtleties of X-ray diffraction on this system, see Ref. [138]; for aspects related to the microstructure studied by X-ray microscopy and micro-NEXAXS including dichroism, see Ref. [145].

In addition to the above cases (PHJ and BHJ), other (intermediate) possible architectures have been studied, for example, mixed layers sandwiched between pure layers (planar-mixed heterojunction, PM-HJ) [49]. The impact of the organic–organic architecture on device performance has also been studied. These issues are discussed in, for example, in OPV cells using the rather promising new donor–acceptor pair of DIP and C_{60} as PHJ versus BHJ versus PM-HJ geometry, together with X-ray, AFM, optical, and electronic characterization [49]. For other work on organic–organic heterostructures combining structural and spectroscopic characterization with transport or other device performance parameters, we refer to Refs [146–149] and references therein and of course other chapters in this book.

1.8
Summary and Conclusions

This chapter does not claim to be complete in any way. We have rather presented a few case studies, which we hope serve to highlight a few of the issues specific to the growth of organic thin films. We shall summarize some of these.

1) Epitaxial relations can be complicated, and the films can exhibit a large number of symmetry-equivalent domains. Moreover, the coexistence of different phases can give rise to complications.
2) Islanding (after some critical thickness) is not uncommon, and is, of course, not prevented by well-defined structural relation between film and substrate.
3) Even for systems that tend to “wet” the substrate, overproportional roughening may occur, and the growth exponents may be very different from those expected based on conventional theories.
4) The controlled preparation of organic-based heterostructures can be particularly difficult, given the tendency for interdiffusion of, for example, metal contacts.
5) The growth of organic–organic heterostructures, whether A-on-B or A-mixed-with-B or other architectures, can be a complex endeavor, but offers many ways to further manipulate and engineer device performance.

Despite the “additional complications” of organics, well-ordered thin films can be grown by OMBD. We hope the improvement of the understanding of the growth mechanisms will further promote the applications of organics.

Moreover, organics with their specific features promise to give rise to fundamentally new growth phenomena such as orientational transitions and new universality classes (scaling exponents), which is an exciting subject in its own right.

Acknowledgments

We wish to thank the many students, collaborators, and colleagues who contributed in various ways to the work reviewed here. Valuable comments on the manuscript were made by A. Gerlach, S. Kowarik, W. Brütting, and J. Pflaum. We wish to acknowledge financial support from the Deutsche Forschungsgemeinschaft.

References

1 Romaner, L., Heimel, G., Bredas, J.L., Gerlach, A., Schreiber, F., Johnson, R.L., Zegenhagen, J., Duhm, S., Koch, N., and Zojer, E. (2007) *Phys. Rev. Lett.*, **99**, 256801.

2 Yamane, H., Gerlach, A., Duhm, S., Tanaka, Y., Hosokai, T., Mi, Y., Zegenhagen, J., Koch, N., Seki, K., and Schreiber, F. (2010) *Phys. Rev. Lett.*, **105**, 046103.

3 Koma, A. (1995) *Prog. Cryst. Growth Charact.*, **30**, 129.

4 Umbach, E., Sokolowski, S., and Fink, R. (1996) *Appl. Phys. A*, **63**, 565.

5 Forrest, S.R. (1997) *Chem. Rev.*, **97**, 1793.

6 Karl, N. and Günther, C. (1999) *Cryst. Res. Technol.*, **34**, 243.

7 Hooks, D.E., Fritz, T., and Ward, M.D. (2001) *Adv. Mater.*, **13**, 227.

8 Fraxedas, J. (2002) *Adv. Mater.*, **14**, 1603.

9 Dimitrakopoulos, C.D. and Malenfant, P. R.L. (2002) *Adv. Mater.*, **14**, 99.

10 Rosei, F., Schunack, M., Naitoh, Y., Jiang, P., Gourdon, A., Laegsgaard, E., Stensgaard, I., Joachim, C., and Besenbacher, F. (2003) *Prog. Surf. Sci.*, **71**, 95.

11 Barlow, S.M. and Raval, R. (2003) *Surf. Sci. Rep.*, **50**, 201.

12 Witte, G. and Wöll, C. (2004) *J. Mater. Res.*, **19**, 1889.

13 Schreiber, F. (2004) *Phys. Stat. Sol. (a)*, **201**, 1037.

14 Gerlach, A., Sellner, S., Kowarik, S., and Schreiber, F. (2008) *Phys. Stat. Sol. (a)*, **205**, 461.

15 Kowarik, S., Gerlach, A., and Schreiber, F. (2008) *J. Phys. Condens. Matter*, **20**, 184005.

16 Lorenzo, M.O., Baddeley, C.J., Muryn, C., and Raval, R. (2000) *Nature*, **404**, 376.

17 Shen, Q., Frankel, D., and Richardson, N.V. (2002) *Surf. Sci.*, **497**, 37.

18 Toomes, R.L., Kang, J.H., Woodruff, D. P., Polcik, M., Kittel, M., and Hoeft, J.T. (2003) *Surf. Sci. Lett.*, **522**, L9.

19 Kowarik, S., Gerlach, A., Sellner, S., Schreiber, F., Cavalcanti, L., and Konovalov, O. (2006) *Phys. Rev. Lett.*, **96**, 125504.

20 Barabási, A.-L. and Stanley, H.E. (1995) *Fractal Concepts in Surface Growth*, Cambridge University Press, Cambridge.

21 Krim, J. and Palasantzas, G. (1995) *Int. J. Mod. Phys. B*, **9**, 599.

22 Krug, J. (1997) *Adv. Phys.*, **46**, 139.

23 Pimpinelli., A. and Villain, J. (1999) *Physics of Crystal Growth*, Cambridge University Press, Cambridge.

24 Biscarini, F., Samori, P., Greco, O., and Zamboni, R. (1997) *Phys. Rev. Lett.*, **78**, 2389.

25 Dürr, A.C., Schreiber, F., Ritley, K.A., Kruppa, V., Krug, J., Dosch, H., and Struth, B. (2003) *Phys. Rev. Lett.*, **90**, 016104.

26 Glöckler, K., Seidel, C., Soukopp, A., Sokolowski, M., Umbach, E., Böhringer, M., Berndt, R., and Schneider, W.-D. (1998) *Surf. Sci.*, **405**, 1.

27 Möbus, M., Karl, N., and Kobayashi, T. (1992) *J. Cryst. Growth*, **116**, 495.

28 Fenter, P., Schreiber, F., Zhou, L., Eisenberger, P., and Forrest, S.R. (1997) *Phys. Rev. B*, **56**, 3046.

29 Seidel, C., Awater, C., Liu, X.D., Ellerbrake, R., and Fuchs, H. (1997) *Surf. Sci.*, **371**, 123.

30 Krause, B., Dürr, A.C., Ritley, K., Schreiber, F., Dosch, H., and Smilgies, D. (2002) *Phys. Rev. B*, **66**, 235404.

31 Krause, B., Dürr, A.C., Schreiber, F., Dosch, H., and Seeck, O.H. (2003) *J. Chem. Phys.*, **119**, 3429.

32 Krause, B., Dürr, A.C., Ritley, K.A., Schreiber, F., Dosch, H., and Smilgies, D. (2001) *Appl. Surf. Sci.*, **175**, 332.

33 Schmitz-Hübsch, T., Fritz, T., Sellam, F., Staub, R., and Leo, K. (1997) *Phys. Rev. B*, **55**, 7972.

34 Hoffmann, M., Schmidt, K., Fritz, T., Hasche, T., Agranovich, V.M., and Leo, K. (2000) *Chem. Phys.*, **258**, 73.

35 Leonhardt, M., Mager, O., and Port, H. (1999) *Chem. Phys. Lett.*, **313**, 24.

36 Vragović, I., Scholz, R., and Schreiber, M. (2002) *Europhys. Lett.*, **57**, 288.

37 Alonso, M.I., Garriga, M., Karl, N., Ossó, J.O., and Schreiber, F. (2002) *Org. Electron.*, **3**, 23.

38 Scholz, R. (2003) Habilitation Thesis, Chemnitz.

39 Scholz, R., Kobitski, A.Y., Kampen, T.U., Schreiber, M., Zahn, D.R.T., Jungnickel, G., Elstner, M., Sternberg, M., and Frauenheim, T. (2000) *Phys. Rev. B*, **61**, 13659.

40 Tautz, F.S., Sloboshanin, S., Schaefer, J. A., Scholz, R., Shklover, V., Sokolowski, M., and Umbach, E. (2000) *Phys. Rev. B*, **61**, 16933.

41 Wagner, V., Muck, T., Geurts, J., Schneider, M., and Umbach, E. (2003) *Appl. Surf. Sci.*, **212**, 520.

42 Dürr, A.C., Schreiber, F., Münch, M., Karl, N., Krause, B., Kruppa, V., and Dosch, H. (2002) *Appl. Phys. Lett.*, **81**, 2276.

43 Dürr, A.C., Koch, N., Kelsch, M., Rühm, A., Ghijsen, J., Johnson, R.L., Pireaux, J. J., Schwartz, J., Schreiber, F., Dosch, H., and Kahn, A. (2003) *Phys. Rev. B*, **68**, 115428.

44 Dürr, A.C., Schreiber, F., Kelsch, M., and Dosch, H. (2003) *Ultramicroscopy*, **98**, 51.

45 Karl, N. (2001) *Organic Electronic Materials*, vol. **2** (eds R. Farchioni and G. Grosso), Springer, Berlin.

46 Kurrle, D. and Pflaum, J. (2008) *Appl. Phys. Lett.*, **92**, 133306.

47 Heinemeyer, U., Scholz, R., Gisslén, L., Alonso, M.I., Ossó, J.O., Garriga, M., Hinderhofer, A., Kytka, M., Kowarik, S., Gerlach, A., and Schreiber, F. (2008) *Phys. Rev. B*, **78**, 085210.

48 Scholz, R., Gisslen, L., Schuster, B.-E., Casu, M.B., Chassé, T., Heinemeyer, U., and Schreiber, F. (2011) *J. Chem. Phys.*, **134**, 014504.

49 Wagner, J., Gruber, M., Hinderhofer, A., Wilke, A., Bröker, B., Frisch, J., Amsalem, P., Vollmer, A., Opitz, A., Koch, N., Schreiber, F., and Brütting, W. (2010). *Adv. Funct. Mater.*, **20**, 4295.

50 Lippel, P.H., Wilson, R.J., Miller, M.D., Wöll, C., and Chiang, S. (1989) *Phys. Rev. Lett.*, **62**, 171.

51 Leznoff, C.C. and Lever, A.B.P. (1989) *Phthalocyanines: Properties and Applications*, VCH Publishers Inc., New York.

52 Schlettwein, D. (2001) *Supramolecular Photosensitive and Electroactive Materials* (ed. H.S. Nalwa), Academic Press, San Diego.

53 Yim, S. and Jones, T.S. (2002) *Surf. Sci.*, **521**, 151.

54 Alonso, M.I., Garriga, M., Ossó, J.O., Schreiber, F., Barrena, E., and Dosch, H. (2003) *J. Chem. Phys.*, **119**, 6335.

55 Rogers, J.A., Bao, Z., Dodabalapur, A., and Makhija, A. (2000) *IEEE Electron. Dev. Lett.*, **21**, 100.

56 Bao, Z., Lovinger, A.J., and Brown, J. (1998) *J. Am. Chem. Soc.*, **120**, 207.

57 Inoue, Y., Sakamoto, Y., Suzuki, T., Kobayashi, M., Gao, Y., and Tokito, S. (2005) *Jpn. J. Appl. Phys. 1*, **44**, 3663.

58 Hinderhofer, A., Heinemeyer, U., Gerlach, A., Kowarik, S., Jacobs, R.M. J., Sakamoto, Y., Suzuki, T., and Schreiber, F. (2007) *J. Chem. Phys.*, **127**, 194705.

59 Koch, N., Vollmer, A., Duhm, S., Sakamoto, Y., and Suzuki, T. (2007) *Adv. Mater.*, **19**, 112.

60 Kowarik, S., Gerlach, A., Hinderhofer, A., Milita, S., Borgatti, F., Zontone, F., Suzuki, T., Biscarini, F., and Schreiber, F. (2008) *Phys. Stat. Sol. (RRL)*, **2**, 120.

61 Desai, T.V., Woll, A.R., Schreiber, F., and Engstrom, J.R. (2010) *J. Phys. Chem. C*, **114**, 20120.

62 Schreiber, F. (2004) *J. Phys. Condens. Matter*, **16**, R881.

63 Schreiber, F. (2000) *Prog. Surf. Sci.*, **65**, 151.

64 Shtein, M., Mapel, J., Benziger, J.B., and Forrest, S.R. (2002) *Appl. Phys. Lett.*, **81**, 268.

65 Möbus, M. and Karl, N. (1992) *Thin Solid Films*, **215**, 213.

66 Dürr, A.C., Schreiber, F., Kelsch, M., Carstanjen, H.D., and Dosch, H. (2002) *Adv. Mater.*, **14**, 961.

67 Dürr, A.C., Schreiber, F., Kelsch, M., Carstanjen, H.D., Dosch, H., and Seeck, O.H. (2003) *J. Appl. Phys.*, **93**, 5201.

68 Koch, N., Dürr, A.C., Ghijsen, J., Johnson, R.L., Pireaux, J.J., Schwartz, J., Schreiber, F., Dosch, H., and Kahn, A. (2003) *Thin Solid Films*, **441**, 145.

69 Heinemeyer, U., Broch, K., Hinderhofer, A., Kytka, M., Scholz, R., Gerlach, A., and Schreiber, F. (2010) *Phys. Rev. Lett.*, **104**, 257401.

70 Zhang, D., Heinemeyer, U., Stanciu, C., Sackrow, M., Braun, K., Hennemann, L. E., Wang, X., Scholz, R., Schreiber, F., and Meixner, A.J. (2010) *Phys. Rev. Lett.*, **104**, 056601.

71 Krug, J. (1995) *Phys. Rev. Lett.*, **75**, 1795.

72 Kowarik, S., Gerlach, A., Skoda, M., Sellner, S., and Schreiber, F. (2009) *Eur. Phys. J. Special Topics*, **167**, 11.

73 Ossó, J.O., Schreiber, F., Alonso, M.I., Garriga, M., Barrena, E., and Dosch, H. (2004) *Org. Electron.*, **5**, 135.

74 de Oteyza, D., Barrena, E., Osso, J., Sellner, S., Dosch, H. (2006) *J. Am. Chem. Soc.*, **128**15052.

75 Hosokai, T., Gerlach, A., Hinderhofer, A., Frank, C., Ligorio, G., Heinemeyer, U., Vorobiev, A., and Schreiber, F. (2010) *Appl. Phys. Lett.*, **97**, 063301.

76 Yim, S. and Jones, T.S. (2006) *Phys. Rev. B*, **73**, 161305.

77 Ruiz, R., Nickel, B., Koch, N., Feldman, L.C., Haglund, R., Jr., Kahn, A., Family, F., and Scoles, G. (2003) *Phys. Rev. Lett.*, **91**, 136102.

78 Meyer zu Heringdorf, F.-J., Reuter, M.C., and Tromp, R.M. (2001) *Nature*, **412**, 517.

79 Nickel, B., Barabash, R., Ruiz, R., Koch, N., Kahn, A., Feldman, L.C., Haglund, R. F., and Scoles, G. (2004) *Phys. Rev. B*, **70**, 125401.

80 Mayer, A., Kazimirov, A., and Malliaras, G. (2006) *Phys. Rev. Lett.*, **97**, 105503.

81 Kowarik, S., Gerlach, A., Leitenberger, W., Hu, J., Witte, G., Wöll, C., Pietsch, U., and Schreiber, F. (2007) *Thin Solid Films*, **515**, 5606.

82 Voigt, M., Dorsfeld, S., Volz, A., and Sokolowski, M. (2003) *Phys. Rev. Lett.*, **91**, 026103.

83 Becker, T., Birkner, A., Witte, G., and Wöll, C. (2002) *Phys. Rev. B*, **65**, 115401.

84 Ossó, J.O., Schreiber, F., Kruppa, V., Dosch, H., Garriga, M., Alonso, M.I., and Cerdeira, F. (2002) *Adv. Funct. Mater.*, **12**, 455.

85 Schreiber, F., Gerstenberg, M.C., Dosch, H., and Scoles, G. (2003) *Langmuir*, **19**, 10004.

86 Schreiber, F., Gerstenberg, M.C., Edinger, B., Toperverg, B., Forrest, S.R., Scoles, G., and Dosch, H. (2000) *Phys. B*, **283**, 75.

87 Gerstenberg, M.C., Schreiber, F., Leung, T.Y.B., Bracco, G., Forrest, S.R., and Scoles, G. (2000) *Phys. Rev. B*, **61**, 7678.

88 Staub, R., Toerker, M., Fritz, T., Schmitz-Hübsch, T., Sellam, F., and Leo, K. (2000) *Surf. Sci.*, **445**, 368.

89 Eremtchenko, M., Schaefer, J., and Tautz, F.S. (2003) *Nature*, **425**, 602.

90 Hauschild, A., Karki, K., Cowie, B.C.C., Rohlfing, M., Tautz, F.S., and Sokolowski, M. (2005) *Phys. Rev. Lett.*, **94**, 036106.

91 Gerlach, A., Sellner, S., Schreiber, F., Koch, N., and Zegenhagen, J. (2007) *Phys. Rev. B*, **75**, 045401.

92 Tautz, F.S. (2007) *Prog. Surf. Sci.*, **82**, 479.

93 Ziroff, J., Forster, F., Schöll, A., Puschnig, P., and Reinert, F. (2010) *Phys. Rev. Lett.*, **104**, 233004.

94 Chizhov, I., Kahn, A., and Scoles, G. (2000) *J. Cryst. Growth*, **208**, 449.

95 Henze, S.K.M., Bauer, O., Lee, T.-L., Sokolowski, M., and Tautz, F.S. (2007) *Surf. Sci.*, **601**, 1566.

96 Duhm, S., Gerlach, A., Salzmann, I., Bröcker, B., Johnson, R., Schreiber, F., and Koch, N. (2008) *Org. Electron.*, **9**, 111.

97 Seidel, C., Poppensieker, J., and Fuchs, H. (1998) *Surf. Sci.*, **408**, 223.

98 Stöhr, M., Gabriel, M., and Möller, R. (2002) *Europhys. Lett.*, **59**, 423.

99 Stöhr, M., Gabriel, M., and Möller, R. (2002) *Surf. Sci.*, **507–510**, 330.

100 Gabriel, M., Stöhr, M., and Möller, R. (2002) *Appl. Phys. A*, **74**, 303.

101 Chkoda, L., Schneider, M., Shklover, V., Kilian, L., Sokolowski, M., Heske, C., and Umbach, E. (2003) *Chem. Phys. Lett.*, **371**, 548.

102 Krause, B., Schreiber, F., Dosch, H., Pimpinelli, A., and Seeck, O.H. (2004) *Europhys. Lett.*, **65**, 372.

103 Fenter, P., Schreiber, F., Bulovic, V., and Forrest, S.R. (1997) *Chem. Phys. Lett.*, **277**, 521.

104 Ritley, K.A., Krause, B., Schreiber, F., and Dosch, H. (2001) *Rev. Sci. Instrum.*, **72**, 1453.

105 Fenter, P., Eisenberger, P., Burrows, P., Forrest, S.R., and Liang, K.S. (1996) *Phys. B*, **221**, 145.

106 Marchetto, H., Groh, U., Schmidt, T., Fink, R., Freund, H.-J., and Umbach, E. (2006) *Chem. Phys.*, **325**, 178184.

107 Krause, B., Dürr, A.C., Schreiber, F., Dosch, H., and Seeck, O.H. (2004) *Surf. Sci.*, **572**, 385.

108 Strohmaier, R.PhD thesis, Stuttgart (1997)

109 Casu, M.B., Schuster, B.-E., Biswas, I., Raisch, C., Marchetto, H., Schmidt, T., and Chassé, T. (2010) *Adv. Mater.*, **22**, 3740.

110 Huang, H., Huang, Y., Pflaum, J., Wee, A.T.S., and Chen, W. (2009) *Appl. Phys. Lett.*, **95**, 263309.

111 Gerlach, A., Schreiber, F., Sellner, S., Dosch, H., Vartanyants, I.A., Cowie, B.C. C., Lee, T.-L., and Zegenhagen, J. (2005) *Phys. Rev. B*, **71**, 205425.

112 Stadler, C., Hansen, S., Pollinger, F., Kumpf, C., Umbach, E., Lee, T.-L., and Zegenhagen, J. (2006) *Phys. Rev. B*, **74**, 035404.

113 Peisert, H., Schwieger, T., Auerhammer, J.M., Knupfer, M., Golden, M.S., Fink, J., Bressler, P.R., and Mast, M. (2001) *J. Appl. Phys.*, **90**, 466.

114 Yannoulis, P., Dudde, R., Frank, K.H., and Koch, E.E. (1987) *Surf. Sci.*, **189/190**, 519.

115 France, C.B., Schroeder, P.G., Forsythe, J. C., and Parkinson, B.A. (2003) *Langmuir*, **19**, 1274.

116 Käfer, D., Ruppel, L., and Witte, G. (2007) *Phys. Rev. B*, **75**, 085309.

117 Koch, N., Gerlach, A., Duhm, S., Glowatzki, H., Heimel, G., Vollmer, A., Sakamoto, Y., Suzuki, T., Zegenhagen, J., Rabe, J.P., and Schreiber, F. (2008) *J. Am. Chem. Soc.*, **130**, 7300.

118 Lukas, S., Witte, G., and Wöll, C. (2002) *Phys. Rev. Lett.*, **88**, 028301.

119 Lukas, S., Söhnchen, S., Witte, G., and Wöll, C. (2004) *Chem. Phys. Chem*, **5**, 266.

120 Casalis, L., Danisman, M.F., Nickel, B., Bracco, G., Toccoli, T., Iannotta, S., and Scoles, G. (2003) *Phys. Rev. Lett.*, **90**, 206101.

121 Kera, S., Yamane, H., Fukagawa, H., Hanatani, T., Okudaira, K.K., Seki, K., and Ueno, N. (2007) *J. Electron. Spectrosc. Relat. Phenom.*, **156**, 135.

122 Proehl, H., Dienel, T., Nitsche, R., and Fritz, T. (2004) *Phys. Rev. Lett.*, **93**, 097403.

123 Brinkmann, M., Graff, S., Straupé, C., Wittmann, J.-C., Chaumont, C., Nuesch, F., Aziz, A., Schaer, M., and Zuppiroli, L. (2003) *J. Phys. Chem. B*, **107**, 10531.

124 Okazaki, N. and Sambles, J.R. (2000) Extended Abstr. Int. Symp. Org. Mol. Electron. (Nagoya, Japan), May 18–19 pp. 66–67.

125 Faupel, F., Willecke, R., and Thran, A. (1998) *Mater. Sci. Eng.*, **R22**, 1.

126 Scharnberg, M., Hu, J., Kanzow, J., Ratzke, K., Adelung, R., Faupel, F., Pannemann, C., Hilleringmann, U., Meyer, S., and Pflaum, J. (2005) *Appl. Phys. Lett.*, **86**, 024104.

127 Sellner, S., Gerlach, A., Schreiber, F., Kelsch, M., Kasper, N., Dosch, H., Meyer, S., Pflaum, J., Fischer, M., and Gompf, B. (2004) *Adv. Mater.*, **16**, 1750.

128 Sellner, S., Gerlach, A., Schreiber, F., Kelsch, M., Kasper, N., Dosch, H., Meyer, S., Pflaum, J., Fischer, M., Gompf, B., and Ulbricht, G. (2006) *J. Mater. Res.*, **16**, 1750.

129 So, F.F., Forrest, S.R., Shi, Y.Q., and Steier, W.H. (1990) *Appl. Phys. Lett.*, **56**, 674.

130 Anderson, M.L., Williams, V.S., Schuerlein, T.J., Collins, G.E., England, C.D., Chau, L.-K., Lee, P.A., Nebesny, K. W., and Armstrong, N.R. (1994) *Surf. Sci.*, **307–309**, 551.

131 Akimichi, H., Inoshita, T., Hotta, S., Noge, H., and Sakaki, H. (1993) *Appl. Phys. Lett.*, **63**, 3158.

132 Nonaka, T., Mori, Y., Nagai, N., Nakagawa, Y., Saeda, M., Takahagi, T., and Ishitani, A. (1994) *Thin Solid Films*, **239**, 214.

133 Sellam, F., Schmitz-Hübsch, T., Toerker, M., Mannsfeld, S., Proehl, H., Fritz, T., Leo, K., Simpson, C., and Müllen, K. (2001) *Surf. Sci.*, **478**, 113.

134 Hoshino, A., Isoda, S., and Kobayashi, T. (1991) *J. Cryst. Growth*, **115**, 826.

135 Heutz, S., Salvan, G., Jones, T.S., and Zahn, D.R.T. (2003) *Adv. Mater.*, **15**, 1109.

136 Hinderhofer, A., and Schreiber, F. (2012) Organic-organic heterostructures: Concepts and applications. *Chem. Phys. Chem.* **13**, 628.

137 Hinderhofer, A., Gerlach, A., Kowarik, S., Zontone, F., Krug, J., and Schreiber, F. (2010) *Europhys. Lett.*, **91**, 56002.

138 Barrena, E., de Oteyza, D.G., Sellner, S., Dosch, H., Ossol, J.O., and Struth, B. (2006) *Phys. Rev. Lett.*, **97**, 076102.

139 Hinderhofer, A., Frank, C., Hosokai, T., Resta, A., Gerlach, A., and Schreiber, F. (2011). Structure and morphology of co-evaporated pentacene-perfluoropentacene thin films. *J. Chem. Phys.* **134**, 104702.

140 Vogel, J.-O., Salzmann, I., Duhm, S., Oehzelt, M., Rabe, J.P., and Koch, N. (2010) *J. Mater. Chem.*, **20**, 4055.

141 Salzmann, I., Duhm, S., Heimel, G., Rabe, J.P., Koch, N., Oehzelt, M., Sakamoto, Y., and Suzuki, T. (2008) *Langmuir*, **24**, 7294.

142 Salzmann, I., Duhm, S., Heimel, G., Oehzelt, M., Kniprath, R., Johnson, R.L., Rabe, J.P., and Koch, N. (2008) *J. Am. Chem. Soc.*, **130**, 12870.

143 Broch, K., Heinemeyer, U., Hinderhofer, A., Anger, F., Scholz, R., Gerlach, A., and Schreiber, F. (2011) Optical evidence for intermolecular coupling in mixed films of pentacene and perfluoropentacene. *Phys. Rev. B*, **83**, 245307.

144 Anger, F., Ossó, J. O., Heinemeyer, U., Broch, K., Scholz, R., Gerlach, A., and Schreiber, F. (2012) Photoluminescence spectroscopy of pure pentacene, perfluoropentacene and mixed thin films. *J. Chem. Phys.* **136**, 054701.

145 Kowarik, S., Broch, K., Hinderhofer, A., Schwartzberg, A., Ossó, J.O., Kilcoyne, D., Schreiber, F., and Leone, S.R. (2010) *J. Phys. Chem. C*, **114**, 13061.

146 Opitz, A., Ecker, B., Wagner, J., Hinderhofer, A., Schreiber, F., Manara, J., Pflaum, J., and Brütting, W. (2009) *Org. Electron.*, **10**, 1259.

147 Opitz, A., Wagner, J., Ecker, B., Hörmann, U., Kraus, M., Bronner, M., Brütting, W., Hinderhofer, A., and Schreiber, F. (2009) *Mater. Res. Soc. Proc.*, **1154**, 9.

148 Opitz, A., Wagner, J., Brütting, W., Hinderhofer, A., and Schreiber, F. (2009) *Phys. Stat. Sol. (a)*, **206**, 2683.

149 Opitz, A., Wagner, J., Brütting, W., Salzmann, I., Koch, N., Manara, J., Pflaum, J., Hinderhofer, A., and Schreiber, F. (2010) *IEEE J. Sel. Top. Quant.*, **99**, 1.